Langmuir
Letter
pubs.acs.org/Langmuir

Monolayer-Protected Gold Nanoparticles Prepared Using Long-Chain Alkanethioacetates†

Shishan Zhang, Gyu Leem, and T. Randall Lee*

Departments of Chemistry and Chemical Engineering, University of Houston, 4800 Calhoun Road, Houston, Texas 77204-5003

Received May 23, 2009. Revised Manuscript Received June 25, 2009

This letter describes the preparation of monolayer-protected nanoparticle clusters (MPCs) from the adsorption of *n*-tetradecanethioacetate onto colloidal gold nanoparticles using the Brust−Schiffrin two-phase synthesis method. The MPCs were characterized by transmission electron microscopy (TEM), ultraviolet−visible (UV−vis) spectroscopy, ^{1}H nuclear magnetic resonance (NMR) spectroscopy, X-ray photoelectron spectroscopy (XPS), and Fourier transform infrared (FTIR) spectroscopy. These studies found that the monolayer coatings on the gold nanoparticles were nearly indistinct with regard to chemical composition, monolayer structure, and Au−S ligation when compared to those prepared from the analogous adsorption of *n*-tetradecanethiol (i.e., the thioacetate headgroup adsorbs to gold as a thiolate, with concurrent loss of the acetyl group). Under equivalent conditions of formation, however, the size of the gold nanoparticles formed was larger when using the alkanethioacetate adsorbate (e.g., 4.9 ± 1.2 nm) compared to the alkanethiol adsorbate (e.g., 1.6 ± 0.3 nm). The observed difference in size is rationalized on the basis of the stronger ligating ability of the thiol compared to that of the thioacetate during gold nanoparticle nucleation and/or growth. The use of alkanethioacetates affords significant control of particle size and allows the formation of MPCs with thiol-sensitive ω-functional groups.

Introduction

Self-assembled monolayers (SAMs) generated by the spontaneous assembly of organic molecules on two-dimensional (2-D) substrates are widely used in a variety of technological applications.[1,2] The process of self-assembly is associated with the spontaneous adsorption and organization of an active surfactant-like species on a solid surface and therefore includes a variety of adsorbates and substrates, such as phosphines on platinum or palladium,[3−5] silanes on silica,[6,7] and thiols on gold, silver, and copper.[8] Research involving SAMs on flat substrates has been adapted to form three-dimensional (3-D) SAM-coated structures, specifically, monolayer-protected nanoparticle clusters (MPCs), which can be handled as isolable species and further functionalized with a variety of reagents.[9] Since the initial description of $Au_{55}(PPh_3)_{12}Cl_6$ by Schmid,[10] researchers have prepared MPCs using a variety of ligands, including thiols, disulfides, dialkyl sulfides, thiosulfates, xanthates, carbamates, phosphines, phosphine oxides, amines, carboxylates, selenides, and isocyanides.[11] Furthermore, the use of the Brust−Schiffrin[12] two-phase synthesis method now allows facile tailoring of the surface properties of thiolate-functionalized nanoparticles by selecting from structurally diverse alkanethiols or alkyl disulfides having various chain lengths and/or ω-functional groups.[9,13]

Given that the interfacial properties of SAMs are critical in technological applications,[1,2,11] researchers who utilize SAMs have explored various protecting-group strategies[14] in cases where the targeted ω-terminal groups are reactive toward thiols[15] or some intermolecular reactions may occur (e.g., aromatic thiols can easily undergo oxidation to form disulfide in the presence of a small amount of oxygen).[16] Notably, several research groups[17−19] have successfully utilized the *S*-acetyl-protected species in the formation of 2-D SAMs on flat gold substrates. In these studies, the direct attachment of adsorbates via their terminal thioacetate group was also observed; like SAMs derived from alkanethiols, the adsorbed sulfur species were thiolates. For the alkanethioacetate system, however, SAM formation occurred less readily than with analogous thiol-terminated adsorbates. In light of these studies, we were surprised to find no reports of the use of thioacetate-terminated adsorbates to prepare 3-D SAMs on colloidal substrates.

Alkanethioacetates can be readily prepared from mesylate- or halo-functionalized organic precursors. The preparation of

† Part of the "Langmuir 25th Year: Nanoparticles synthesis, properties, and assemblies" special issue.

*To whom correspondence should be addressed. E-mail: trlee@uh.edu.

(1) Love, J. C.; Estroff, L. A.; Kriebel, J. K.; Nuzzo, R. G.; Whitesides, G. M. *Chem. Rev.* **2005**, *105*, 1103.
(2) Ulman, A. *Chem. Rev.* **1996**, *96*, 1533.
(3) Mallat, T.; Broennimann, C.; Baiker, A. *Appl. Catal.* **1997**, *149*, 103.
(4) Mitchell, G. E.; Henderson, M. A.; White, J. M. *J. Phys. Chem.* **1987**, *91*, 3808.
(5) Ugo, R. *Coord. Chem. Rev.* **1968**, *3*, 319.
(6) Gun, J.; Iscovici, R.; Sagiv, J. *J. Colloid Interface Sci.* **1984**, *101*, 201.
(7) Wasserman, S. R.; Tao, Y. T.; Whitesides, G. M. *Langmuir* **1989**, *5*, 1074.
(8) Laibinis, P. E.; Whitesides, G. M. *J. Am. Chem. Soc.* **1992**, *114*, 9022.
(9) Templeton, A. C.; Wuelfing, W. P.; Murray, R. W. *Acc. Chem. Res.* **2000**, *33*, 27.
(10) Schmid, G.; Pfeil, R.; Boese, R.; Bandermann, F.; Meyer, S.; Calis, G. H. M.; van der Velden, J. A. W. *Chem. Ber.* **1981**, *114*, 3634.
(11) Daniel, M.-C.; Astruc, D. *Chem. Rev.* **2004**, *104*, 293.
(12) Brust, M.; Walker, M.; Bethell, D.; Schiffrin, D. J.; Whyman, R. *J. Chem. Soc., Chem. Commun.* **1994**, 801.
(13) Ingram, R. S.; Hostetler, M. J.; Murray, R. W. *J. Am. Chem. Soc.* **1997**, *119*, 9175.
(14) Greene, T. W. *Protective Groups in Organic Synthesis*, 3rd ed.; Wiley: New York, 1999.
(15) Witt, D.; Klajn, R.; Barski, P.; Grzybowski, B. A. *Curr. Org. Chem.* **2004**, *8*, 1763.
(16) Tarbell, D. S. In *Organic Sulfur Compounds*; Kharasch, N., Ed.; Pergamon Press: New York, 1961; Vol. *1*, p 97.
(17) Tour, J. M.; Jones, L. II.; Pearson, D. L.; Lamba, J. J. S.; Burgin, T. P.; Whitesides, G. M.; Allara, D. L.; Parikh, A. N.; Atre, S. *J. Am. Chem. Soc.* **1995**, *117*, 9529.
(18) Kang, Y.; Won, D.-J.; Kim, S. R.; Seo, K.; Choi, H.-S.; Lee, G.; Noh, Z.; Lee, T. S.; Lee, C. *Mater. Sci. Eng., C* **2004**, *C24*, 43.
(19) Béthencourt, M. I.; Srisombat, L.; Chinwangso, P.; Lee, T. R. *Langmuir* **2009**, *25*, 1265.

thioacetate-terminated organic molecules is simpler than that of analogous thiol-terminated organic molecules because the former synthesis requires relatively mild reaction conditions (e.g., no strong reducing agents and/or acidic conditions). Furthermore, nanoparticle growth using the popular Brust−Schiffrin method is believed to proceed via a nucleation−growth−passivation process[9] where the average diameter of the resultant gold nanoparticles becomes smaller when a larger thiol/gold molar ratio is used, the cooled reducing agent is added rapidly, or sterically bulky ligands are involved.[13,20−23] We hypothesized that the use of a weaker binding adsorbate, such as an alkanethioacetate, might prolong the growth processes and thus offer larger nanoparticles than those afforded using standard alkanethiol-based adsorbates.

To this end, this letter describes the preparation and characterization of SAM-protected gold nanoparticles derived using *n*-tetradecanethioacetate as a passivating agent. The results are compared to those obtained via analogous passivation using *n*-tetradecanethiol. The product MPCs were characterized by transmission electron microscopy (TEM), ultraviolet−visible (UV−vis) spectroscopy, ^{1}H nuclear magnetic resonance (^{1}H NMR) spectroscopy, X-ray photoelectron spectroscopy (XPS), and Fourier transform infrared (FTIR) spectroscopy. The studies reveal that the MPCs prepared using *n*-tetradecanethioacetate are markedly larger than those prepared using *n*-tetradecanethiol.

Experimental Section

Materials. Water was purified to a resistance of 18 MΩ using a Milli-Q academic system. All chemicals were used as received from the indicated companies without additional purification: $NaBH_4$, toluene, and hexane (EM Science), $HAuCl_4$ (Strem), absolute ethanol (McKormick Distilling Co.), carbon tetrachloride (CCl_4, Acros), myristyl mercaptan ($C_{14}SH$, TCI), and potassium thioacetate, 1-bromotetradecane, and tetraoctylammonium bromide (TOAB, Aldrich).

Synthesis of the Adsorbates. The thioacetate adsorbate was synthesized following the procedure reported by Evans et al.[24] Potassium thioacetate (1.78 g, 10 mmol) was dissolved in absolute ethanol (100 mL), and the mixture was degassed by bubbling with argon for 30 min. An aliquot of 1-bromo-tetradecane (2.86 g, 10 mmol) was then added, and the solution was refluxed for 12 h. The volatiles were removed by evaporation under vacuum, and the residue was dissolved in water (100 mL) and then extracted with diethyl ether (3 × 100 mL). The combined organic layers were dried over anhydrous magnesium sulfate, filtered, and evaporated under vacuum. The yellowish residue was subjected to column chromatography on silica gel (5% diethyl ether in hexanes) to afford pure *n*-tetradecanethioacetate ($C_{14}SAc$) as a liquid (2.21 g, 8.1 mmol, 81% yield). The structure was confirmed by ^{1}H NMR spectroscopy in $CDCl_3$ using a QE-300 spectrometer.[24]

Preparation of SAM-Protected Gold Nanoparticles Using $C_{14}SH$/$C_{14}SAc$. All glassware used in the preparation and storage of the MPCs was treated with aqua regia, rinsed with water, and cleaned with piranha solution (7:3 concentrated H_2SO_4/30 wt % H_2O_2). (***Caution! Piranha solution reacts violently with organic materials and should be handled with care!***)

Gold nanoparticles coated with $C_{14}SH$ and $C_{14}SAc$ were synthesized in toluene/H_2O in a similar fashion to the work of Brust et al.[12] except that the S/Au mole ratios were maintained at 1:1 and 1:3 in the present work. A 3.0 mL aliquot of a 3×10^{-2} M aqueous solution of $HAuCl_4$ (0.09 mmol) was placed in a 50 mL round-bottomed flask. To this solution, 8.0 mL of a 2.5×10^{-2} M solution of TOAB (0.2 mmol) in toluene was added while stirring vigorously. To provide for complete phase transfer of the gold salt, stirring was continued for at least 15 min. The phase transfer was confirmed visually by observing the disappearance of the pale-yellow color of the aqueous phase and the appearance of the reddish orange color of the organic phase. The adsorbate ($C_{14}SH$ or $C_{14}SAc$; 0.09 mmol) was then added dropwise to the organic phase while stirring. A 7.5 mL aliquot of a freshly prepared 0.1 M aqueous solution of $NaBH_4$ (0.75 mmol) was then added dropwise over 5 min. The mixture was allowed to stir for 24 h. The organic layer was separated using a micropipet, washed with water several times to remove excess TOAB, dried over $MgSO_4$, and concentrated to ca. 1 mL by rotary evaporation. The resulting product was diluted with 50 mL of ethanol and stored at −50 °C overnight. The functionalized gold nanoparticles were then collected as a brownish-black precipitate by centrifugation and were thoroughly rinsed with ethanol (3 × 50 mL).

Control Experiment to Probe the Possible Reduction of Alkanethioacetate by $NaBH_4$. The procedure in the preceding paragraph was performed without the addition of a metal salt ($HAuCl_4$). Separation of the organic and aqueous phases followed by the evaporation of each phase gave in each case a white residue. Each residue was dissolved in $CDCl_3$ and characterized by ^{1}H NMR spectroscopy. No thiol species were detected in the residue containing $C_{14}SAc$ (vide infra).

Characterization of Nanoparticles. TEM images were collected on a JEOL JEM-2010 electron microscope operating at an accelerating bias voltage of 200 kV. Samples were prepared by depositing a film of nanoparticles onto a carbon-coated copper grid. UV−vis spectra were collected using a Cary 50 scan UV−visible extinction spectrometer. All samples were placed in a quartz cuvette having a 1 cm optical path length, and the baseline of each spectrum was corrected by subtracting a spectrum of the corresponding solvent. ^{1}H NMR spectra were recorded on a General Electric QE-300 spectrometer operating at 300 MHz in $CDCl_3$ and internally referenced to 7.26 ppm. XPS spectra were obtained using a PHI 5700 X-ray photoelectron spectrometer equipped with a monochromatic Al Kα X-ray source ($h\nu$ = 1486.7 eV). The spectrometer was operated at high resolution with a pass energy of 23.5 eV, a photoelectron takeoff angle of 45° from the surface, and an analyzer spot diameter of 2 mm. The base pressure in the chamber during measurements was 3×10^{-9} Torr, and the spectra were collected at room temperature. The binding energies of S were referenced to the $Au_{4f7/2}$ peak at 84.0 eV. Infrared spectra were collected using a Nicolet Magna-IR 860 Fourier transform spectrometer. The IR spectra of nanoparticles in solution were collected by dispersing the nanoparticles in carbon tetrachloride and placing an aliquot of the solution between two KBr plates. The IR spectra of nanoparticles in the solid state were collected by depositing an aliquot of the solvent-dispersed nanoparticles on a KBr plate and allowing the solvent to evaporate prior to data collection.

Results and Discussion

Solubilities of $C_{14}SAc$-Functionalized Gold Nanoparticles in Organic Solvents. Gold nanoparticles synthesized using *n*-tetradecanethioacetate as described above were precipitated by centrifugation in ethanol. These SAM-coated nanoparticles could be readily redissolved in a variety of organic solvents, including hexane, toluene, CCl_4, CH_2Cl_2, and THF. Given that bare gold nanoparticles (i.e., those prepared with no SAM coating) typically aggregate in organic solvents,[25] the observed

(20) Leff, D. V.; Ohara, P. C.; Heath, J. R.; Gelbart, W. M. *J. Phys. Chem.* **1995**, *99*, 7036.
(21) Hostetler, M. J.; Stokes, J. J.; Murray, R. W. *Langmuir* **1996**, *12*, 3604.
(22) Chen, S.; Murray, R. W. *Langmuir* **1999**, *15*, 682.
(23) Chen, S. *Langmuir* **1999**, *15*, 7551.
(24) Evans, R. M.; Owen, L. N. *J. Chem. Soc.* **1949**, 244.
(25) Zhu, T.; Vasilev, K.; Kreiter, M.; Mittler, S.; Knoll, W. *Langmuir* **2003**, *19*, 9518.

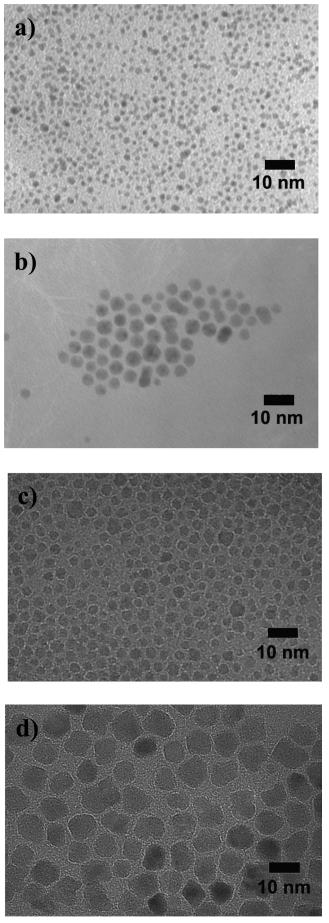

Figure 1. Transmission electron micrographs of SAM-coated gold nanoparticles generated using *n*-tetradecanethiol and *n*-tetradecanethioacetate as passivating agents: (a) *n*-tetradecanethiol, 1:1 S/Au molar ratio; (b) *n*-tetradecanethioacetate, 1:1 S/Au molar ratio; (c) *n*-tetradecanethiol, 1:3 S/Au molar ratio; and (d) *n*-tetradecanethioacetate, 1:3 S/Au molar ratio.

resistance to aggregation here strongly indicates that the alkanethioacetate moieties form at least a partial monolayer on the surface of the gold nanoparticles.

Sizes and Morphologies of C_{14}SH- and C_{14}SAc-Functionalized Gold Nanoparticles. Figure 1a−d shows TEM images of gold nanoparticles synthesized with S/Au molar ratios of 1:1 and 1:3 based on the stoichiometry of the starting reagents. The corresponding statistical analysis of the particle sizes is provided in Figure 2a−d, which demonstrates that the diameters of the nanoparticles are 1.6 ± 0.3 nm (C_{14}SH) and 4.9 ± 1.2 nm (C_{14}SAc) for a 1:1 S/Au molar ratio and 3.2 ± 0.5 nm (C_{14}SH) and 7.2 ± 0.8 nm (C_{14}SAc) for a 1:3 S/Au molar ratio. Two important trends can be drawn from these data: (1) the alkanethioacetate affords significantly larger particles than does the alkanethiol, and (2) a decrease in the S/Au molar ratio gives rise to an increase in the size of the gold nanoparticles. Whereas the latter phenomenon can be rationalized on the basis of the aforementioned nucleation−growth−passivation kinetics model in which the sulfur-containing agents inhibit the growth process,[9,13,20,23,26] the former phenomenon must be attributed to a difference in behavior for the two types of adsorbates, where the thiols are better inhibitors (i.e., stronger ligating agents) than the thioacetates.[17] We note that this trend is consistent with the preferred ligation of

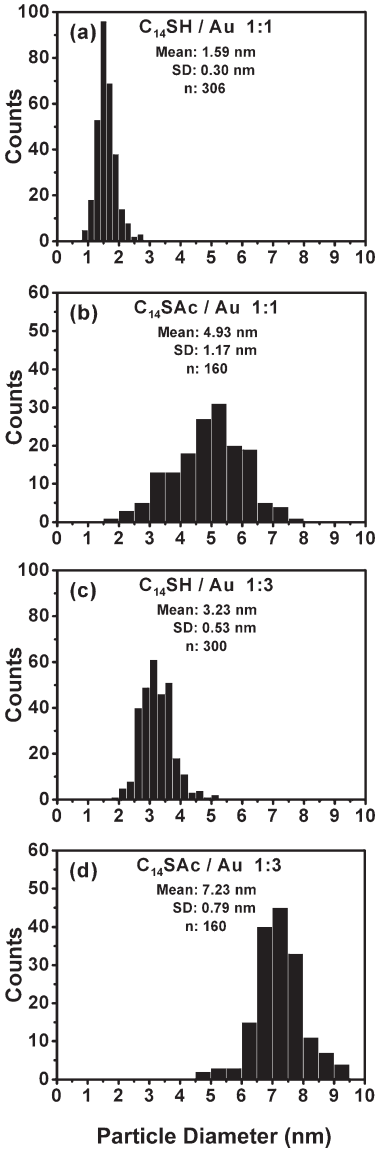

Figure 2. Histograms of the diameters of SAM-coated gold nanoparticles generated using *n*-tetradecanethiol and *n*-tetradecanethioacetate as passivating agents: (a) *n*-tetradecanethiol, 1:1 S/Au molar ratio; (b) *n*-tetradecanethioacetate, 1:1 S/Au molar ratio; (c) *n*-tetradecanethiol, 1:3 S/Au molar ratio; and (d) *n*-tetradecanethioacetate, 1:3 S/Au molar ratio.

thiols versus thioacetates to the surface of gold during SAM formation (i.e., thiols were observed to bind more readily than thioacetates).[17−19] An analogous trend has been observed for dialkyl sulfides[27] and alkanethiosulfates[28] on flat gold as well as dialkyl sulfides[29] and alkanethiosulfates[30] during gold nanoparticle growth. The use of alkanethioacetates affords more stable SAMs and thus more stable MPCs than does the use of dialkyl sulfides (covalent bonding vs dative bonding, respectively).[27,29]

The images in Figure 1 also highlight the morphological features of the gold nanoparticles prepared here. Gold nanoparticles generated at a 1:1 S/Au molar ratio are roughly spherical and

(26) Isaacs, S. R.; Cutler, E. C.; Park, J.-S.; Lee, T. R.; Shon, Y.-S. *Langmuir* **2005**, *21*, 5689.

(27) Troughton, E. B.; Bain, C. D.; Whitesides, G. M.; Nuzzo, R. G.; Allara, D. L.; Porter, M. D. *Langmuir* **1988**, *4*, 365.

(28) Lukkari, J.; Meretoja, M.; Kartio, I.; Laajalehto, K.; Rajamaeki, M.; Lindstroem, M.; Kankare, J. *Langmuir* **1999**, *15*, 3529.

(29) Shelley, E. J.; Ryan, D.; Johnson, S. R.; Couillard, M.; Fitzmaurice, D.; Nellist, P. D.; Chen, Y.; Palmer, R. E.; Preece, J. A. *Langmuir* **2002**, *18*, 1791.

(30) Shon, Y.-S.; Gross, S. M.; Dawson, B.; Porter, M.; Murray, R. W. *Langmuir* **2000**, *16*, 6555.

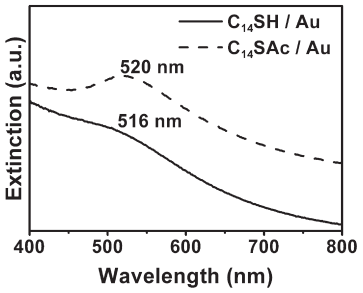

Figure 3. UV−vis spectra of SAM-coated gold nanoparticles in $CHCl_3$ generated using *n*-tetradecanethiol and *n*-tetradecanethioacetate as passivating agents, both at a 1:1 S/Au molar ratio.

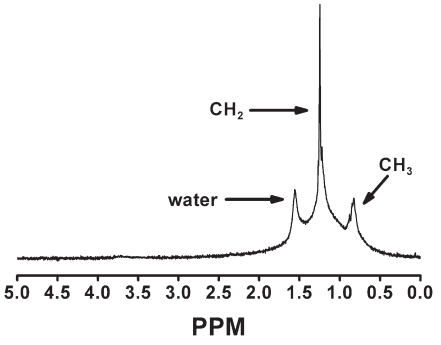

Figure 4. ^{1}H NMR spectrum in $CDCl_3$ of SAM-coated gold nanoparticles generated using *n*-tetradecanethioacetate (1:1 S/Au molar ratio) as a passivating agent.

comparable in appearance to previously reported SAM-coated gold nanoparticles.[31,32] In contrast, gold nanoparticles generated at a 1:3 S/Au molar ratio show some irregular nanocrystals. We believe that the ratio of sulfur to gold is a major factor influencing the morphology of gold nanoparticles.[20]

UV−Vis Spectroscopy of C_{14}SH- and C_{14}SAc-Functionalized Gold Nanoparticles. The UV−vis spectra of the C_{14}SH- and C_{14}SAc-passivated gold nanoparticles in Figure 3 show surface plasmon bands at 516 and 520 nm, respectively, which are consistent with the plasmons reported for gold nanoparticles of the respective sizes functionalized with alkanethiols.[20,33] Importantly, the intensity of the surface plasmon band for the C_{14}SAc-functionalized gold nanoparticles is markedly greater than that for the C_{14}SH-functionalized gold nanoparticles. This observation is consistent with the observed larger size of gold nanoparticles functionalized with C_{14}SAc compared to those functionalized with C_{14}SH (vide supra).[33]

^{1}H NMR Spectroscopy of C_{14}SAc-Functionalized Gold Nanoparticles. ^{1}H NMR spectroscopy is widely employed to characterize MPCs, especially to detect the presence of any free or unbound adsorbates.[13,30,32] Figure 4 shows the ^{1}H NMR spectrum of gold nanoparticles functionalized with *n*-tetradecanethioacetate, which exhibits two broad resonances at 0.8−0.9 and 1.2−1.5 ppm corresponding to methyl and methylene groups, respectively. Similar spectra have been reported for gold nanoparticles functionalized with alkanethiols, dialkyl disulfides, dialkyl sulfides, and alkanethiosulfates.[29,30,32] As with the latter adsorbates, no free alkanethioacetate or related sulfur-based

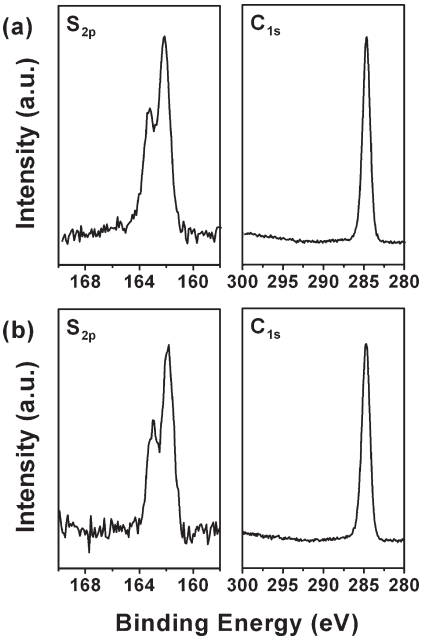

Figure 5. XPS spectra of SAM-coated gold nanoparticles generated using passivating agents (a) *n*-tetradecanethiol and (b) *n*-tetradecanethioacetate, both at a 1:1 S/Au molar ratio.

adsorbate can be detected in the spectrum. This result can be taken to indicate that the hydrocarbon species in the samples are derived from the thioacetate and are attached to the surface of the nanoparticle.[34]

Because alkanethiols are commonly obtained by the reduction of the corresponding alkanethioacetates, it is plausible that some or all of the *n*-tetradecanethioacetate is reduced by $NaBH_4$ to *n*-tetradecanethiol during the two-phase synthesis. In such a case, the transient thiol rather than thioacetate might then serve as the active adsorbate to form the MPCs. To explore this possibility, we performed a two-phase Brust "synthesis" in the absence of any metal salts as a control experiment. During this reaction, we readily detected resonances consistent with *n*-tetradecanethioacetate and tetraoctylammonium bromide in both the aqueous and the organic phases. In contrast, we detected no α-CH_2 resonance at 2.5 ppm corresponding to *n*-tetradecanethiol. Recognizing that there was excess reducing agent in the control experiment and yet no thiol was produced, we conclude that a substantial amount of thiol is not generated from the thioacetate under the reaction conditions. As such, these observations provide strong albeit indirect support that the thioacetate rather than the corresponding thiol is the active sulfur species involved in the formation of SAMs on gold nanoparticles.

XPS of C_{14}SH- and C_{14}SAc-Functionalized Gold Nanoparticles. XPS has been extensively used to analyze both the elemental composition and the oxidation states of the components of MPCs.[35−37] Figure 5a,b shows the photoelectron spectra corresponding to the S 2p and C 1s binding energies of the SAM-coated gold nanoparticles generated using C_{14}SH and C_{14}SAc, respectively. In the S 2p region for both adsorbates, the spectra show photoelectron peaks with binding energies of 162.1 and 163.3 eV, which we assign to the doublet of S $2p_{3/2}$ and S $2p_{1/2}$,

(31) Brust, M.; Fink, J.; Bethell, D.; Schiffrin, D. J.; Kiely, C. *J. Chem. Soc., Chem. Commun.* **1995**, 1655.
(32) Porter, L. A. Jr.; Ji, D.; Westcott, S. L.; Graupe, M.; Czernuszewicz, R. S.; Halas, N. J.; Lee, T. R. *Langmuir* **1998**, *14*, 7378.
(33) Shon, Y.-S.; Mazzitelli, C.; Murray, R. W. *Langmuir* **2001**, *17*, 7735.
(34) Badia, A.; Singh, S.; Demers, L.; Cuccia, L.; Brown, G. R.; Lennox, R. B. *Chem.—Eur. J.* **1996**, *2*, 359.
(35) Buettner, M.; Belser, T.; Oelhafen, P. *J. Phys. Chem. B* **2005**, *109*, 5464.
(36) Johnson, S. R.; Evans, S. D.; Mahon, S. W.; Ulman, A. *Langmuir* **1997**, *13*, 51.
(37) Kang, S. Y.; Kim, K. *Langmuir* **1998**, *14*, 226.

respectively. These binding energies are consistent with a model in which the sulfur species are bound to the surface of gold largely as thiolates (i.e., reduced sulfur species).[38,39] For Figure 5a, we deconvoluted the sulfur spin−orbit doublet using a well-known method[40] that revealed that a small fraction of sulfur atoms exist as unbound thiols (≤10%), giving rise to a peak at 164 eV. This interpretation is consistent with recent studies exploring the use of multidentate thiol-based ligands to fabricate and stabilize small gold nanoparticles.[41] We note, however, that the S 2p spectrum in Figure 5b shows no evidence of *S*-acetyl[42] or oxidized sulfur,[43−45] which normally appear at 163.5 and 167 eV, respectively.

The C 1s region for both adsorbates shows only one peak at a binding energy of 285 eV,[46] which corresponds to the hydrocarbon tail of the adsorbates. In addition, no peaks are present at a binding energy of 286 eV, indicating that there are few or no *S*-acetyl moieties on the surfaces of the nanoparticles.[42] As a whole, these observations offer strong evidence that the MPCs generated using *n*-tetradecanethioacetate have SAM coatings that are chemically similar to those generated using *n*-tetradecanethiol.

IR Spectroscopy of C_{14}SH- and C_{14}SAc-Functionalized Gold Nanoparticles. Infrared spectroscopy has become a useful tool for the determination of structural information concerning organic molecules and their order/assembly in thin-film architectures. Unbound or "free" *n*-tetradanethioacetate exhibits strong IR bands at ∼1100−1135 cm^{-1} and ∼1690−1710 cm^{-1}, which arise from (νC(O)−S)[47,48] and the carbonyl stretch (νC═O),[47−49] respectively. Bonding of the thioacetate to the surface of gold can be followed by observing the loss of these bands, as illustrated in Figure 6. When combined with the results obtained by XPS, this observation provides further support for the thiolate nature of the sulfur atoms in gold-core MPCs prepared using alkanethioacetates.

An examination of the C−H and C−C stretching regions provides information regarding the orientation, order, and packing of the SAMs in MPCs.[13,20,21,34,37] In particular, the degree of conformational order of the alkyl chains can be estimated from the frequency and width of the methylene antisymmetric band ($\nu_a CH_2$).[50−52] Lower frequency and sharper bands

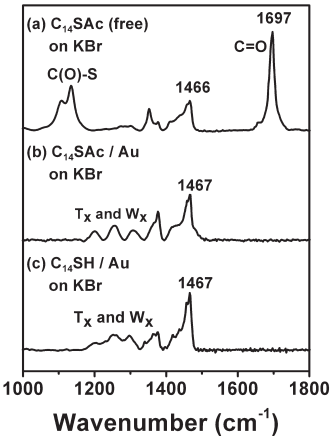

Figure 6. FTIR transmission spectra in the 1000−1800 cm^{-1} region for (a) free *n*-tetradecanethioacetate and solid-state samples of gold nanoparticles functionalized with (b) *n*-tetradecanethioacetate and (c) *n*-tetradecanethiol.

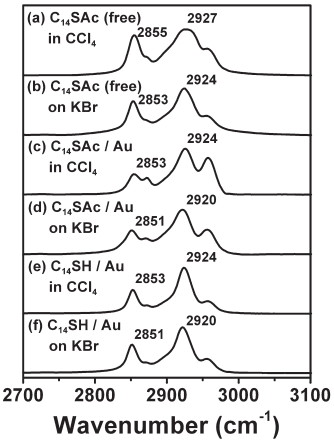

Figure 7. FTIR transmission spectra in the 2700−3100 cm^{-1} region for samples in solution (CCl_4) and in the solid state of (a, b) free *n*-tetradecanethioacetate, (c, d) gold nanoparticles functionalized with *n*-tetradecanehioacetate, and (e, f) gold nanoparticles functionalized with *n*-tetradecanethiol.

are characteristic of chains having a high degree of conformational order. For example, the $\nu_a CH_2$ modes of crystalline polyethylene and *n*-docosanethiol appear as relatively sharp bands at 2920 and 2918 cm^{-1}, which are considered characteristic of an all-trans zigzag conformation, whereas those of liquid polyethylene and liquid *n*-octanethiol appear as broad bands at 2928 and 2924 cm^{-1}, respectively.[50−52]

Figure 7 highlights the C−H stretching region of the following samples both dissolved in CCl_4 and deposited/dried on a KBr substrate: nonadsorbed or "free" *n*-tetradecanethioacetate and gold-core MPCs generated by the adsorption of *n*-tetradecanethioacetate and *n*-tetradecanethiol. We note first that the C−H stretching bands for free *n*-tetradecanethioacetate are indistinct from those of free *n*-tetradecanethiol (not shown). Figure 7a shows the IR spectrum of free *n*-tetradecanethioacetate in CCl_4 solution, where $\nu_a CH_2 = 2927$ cm^{-1} and $\nu_s CH_2 = 2855$ cm^{-1}. In contrast, Figure 7b shows that upon removal of the solvent the corresponding bands sharpen and shift to lower frequency: $\nu_a CH_2 = 2924$ cm^{-1} and $\nu_s CH_2 = 2853$ cm^{-1}. These data indicate that the removal of the solvent increases the conformational order of the methylene chains.

(38) Laibinis, P. E.; Whitesides, G. M.; Allara, D. L.; Tao, Y. T.; Parikh, A. N.; Nuzzo, R. G. *J. Am. Chem. Soc.* **1991**, *113*, 7152.
(39) Lu, H. B.; Campbell, C. T.; Castner, D. G. *Langmuir* **2000**, *16*, 1711.
(40) Zhou, J.; Beattie, D. A.; Sedev, R.; Ralston, J. *Langmuir* **2007**, *23*, 9177.
(41) Srisombat, L.; Park, J. -S.; Zhang, S.; Lee, T. R. *Langmuir* **2008**, *24*, 7750.
(42) Wenzler, L. A.; Moyes, G. L.; Raikar, G. N.; Hansen, R. L.; Harris, J. M.; Beebe, T. P. Jr.; Wood, L. L.; Saavedra, S. S. *Langmuir* **1997**, *13*, 3761.
(43) Badia, A.; Cuccia, L.; Demers, L.; Morin, F.; Lennox, R. B. *J. Am. Chem. Soc.* **1997**, *119*, 2682.
(44) Badia, A.; Demers, L.; Dickinson, L.; Morin, F. G.; Lennox, R. B.; Reven, L. *J. Am. Chem. Soc.* **1997**, *119*, 11104.
(45) Schoenfisch, M. H.; Pemberton, J. E. *J. Am. Chem. Soc.* **1998**, *120*, 4502.
(46) This observation contrasts that observed for SAMs on flat gold derived from thiols and thioacetates having identical chain lengths.[19] During X-ray irradiation of thiol-derived SAMs on flat gold, the positive charges generated by photoelectron emission are not easily dissipated through the well-packed hydrocarbon films, which act as insulators. In contrast, thioacetate-derived SAMs on flat gold are loosely packed and thus are relatively poor insulators, which leads to a distinct shift in the C 1s binding energy when comparing these two types of SAMs. In the present study, however, the SAMs generated by the adsorption of thiols and thioacetates on gold nanoparticles are indistinguishable with respect to conformational order and packing density. Consequently, we observe identical C 1s binding energies for these latter two types of SAMs.
(47) El-Aasar, A. M. M.; Nash, C. P.; Ingraham, L. L. *Biochemistry* **1982**, *21*, 1972.
(48) Marshall, G.; Teer, E.; Knobler, C. M.; Schalke, M.; Losche, M. *Colloids Surf., A* **2000**, *171*, 41.
(49) Olivato, P. R.; Hui, M. L. T.; Rodrigues, A.; Ruiz Filho, R.; Rittner, R.; Zukerman-Schpector, J.; Distefano, G.; Dal Colle, M. *J. Mol. Struct.* **2003**, *645*, 259.
(50) Bensebaa, F.; Ellis, T. H.; Badia, A.; Lennox, R. B. *Langmuir* **1998**, *14*, 2361.
(51) Snyder, R. G.; Strauss, H. L.; Elliger, C. A. *J. Phys. Chem.* **1982**, *86*, 5145.
(52) Porter, M. D.; Bright, T. B.; Allara, D. L.; Chidsey, C. E. D. *J. Am. Chem. Soc.* **1987**, *109*, 3559.

Figure 7c shows the C−H stretching region for the CCl_4-dissolved MPCs generated using *n*-tetradecanethioacetate as the passivating agent, where $\nu_aCH_2 = 2924\ cm^{-1}$ and $\nu_sCH_2 = 2853\ cm^{-1}$. A comparison of these data with those in Figure 7a (free thioacetate in CCl_4) suggests that the adsorption process induces a clearly detectable ordering of the methylene chains. Similarly, Figure 7d shows that evaporation of the solvent further shifts the methylene stretches to $\nu_aCH_2 = 2920\ cm^{-1}$ and $\nu_sCH_2 = 2851\ cm^{-1}$, which indicates a further increase in conformational order reaching a nearly crystalline state. Figure 7e,f shows the analogous IR spectra for CCl_4-dissolved and solid-state MPCs prepared using *n*-tetradecanethiol as the passivating agent. The spectra are indistinguishable from those in Figure 7c,d, which strongly suggests that the conformational order and thus the packing densities of the 3-D SAMs derived from *n*-tetradecanethioacetate are indistinct from those derived from *n*-tetradecanethiol.

As noted previously,[32] the observed enhancement in crystallinity of the tail groups of MPCs upon drying can be attributed to an increase in the chain−chain van der Waals interactions upon the loss of solvent molecules from the SAM matrix. This enhancement can be further confirmed by noting the appearance of twisting−rocking (T_x) and wagging progression (W_x) bands in the 1100−1400 cm^{-1} region (Figure 6). The presence of these progression bands as a series of well-resolved peaks can also be used as an indicator of the degree of crystallinity of SAMs.[21,53,54] We note that the band at 1466 cm^{-1} for the free thioacetate (Figure 6a) can be assigned to the scissoring motion of all-trans methylene chains.[55] For the solid-state SAM-coated MPCs, this band increases in intensisty and shifts to ∼1467 cm^{-1}. The observed increase in band intensity and (albeit small) increase in wavenumber confirm the enhanced crystallinity of the tail groups upon removal of the solvent.

Finally, we note that the methyl group stretches appear markedly more intense for the $C_{14}SAc/Au$ samples than for any of the other samples (Figure 7). This enhancement in intensity does not arise from the thioacetate methyl groups, which should appear roughly at 2929 cm^{-1} (ν_s) and 3003 cm^{-1} (ν_{as}).[47] Instead, the enhancement likely arises from surface selection rules[56] that become important as the gold nanoparticle cores approach bulk dimensions. Notably, the diameters of the $C_{14}SAc/Au$ nanoparticles are roughly twice those of the $C_{14}SH/Au$ nanoparticles, which exhibit no similar enhancement for the methyl stretches when compared to those of the unadsorbed "free" molecules.

Conclusions

These studies have demonstrated that alkanethioacetates can be used as effective passivating agents in the preparation of gold-based MPCs using the Brust−Schiffrin two-phase synthesis method. The resultant MPCs are readily soluble in both polar and nonpolar organic solvents, with solubilities comparable to those prepared analogously using alkanethiols. An analysis of the MPCs by XPS and FTIR shows that the alkanethioacetate-derived SAMs form with the loss of the *S*-acetyl moiety and covalent attachment of the sulfur atoms as thiolates to the surface of gold. Whereas the data collectively demonstrate that the alkanethioacetate-derived monolayer coatings are indistinguishable from those derived from alkanethiols, the use of thioacetates leads to nanoparticles having larger sizes (approximately by a factor of 3) compared to nanoparticles produced by the use of alkanethiols. This difference can be attributed to the weaker ligating ability of thioacetates compared to that of thiols during the growth process. Use of the acetyl protecting group also circumvents disulfide formation and allows the generation of nanoparticles in the presence of thiol-sensitive functional groups.

Acknowledgment. We gratefully acknowledge financial support from the National Science Foundation (ECCS-0926027), the Texas Center for Superconductivity, and the Robert A. Welch Foundation (grant E-1320).

(53) Maroncelli, M.; Qi, S. P.; Strauss, H. L.; Snyder, R. G. *J. Am. Chem. Soc.* **1982**, *104*, 6237.
(54) Smith, E. L.; Porter, M. D. *J. Phys. Chem.* **1993**, *97*, 8032.
(55) Scheuing, D. R.; Weers, J. G. *Colloids Surf.* **1991**, *55*, 41.
(56) Bradshaw, A. M.; Richardson, N. V. *Pure Appl. Chem.* **1996**, *68*, 457.